Power Factor Enhancement for Few-Layered Graphene Films by Molecular Attachments

Daohao Sim,[†] Dayong Liu,[†] Xiaochen Dong,[‡] Ni Xiao,[†] Sean Li,[§] Yang Zhao,[†] Lain-Jong Li,[⊥] Qingyu Yan,[*,†] and Huey Hoon Hng[*,†]

[†]School of Materials Science and Engineering, Nanyang Technological University, 50 Nanyang Avenue, Singapore 639798, Singapore

[‡]Institute of Advanced Materials, Nanjing University of Posts and Telecommunications, 9 Wenyuan Road, Nanjing 210046, People's Republic of China

[§]School of Materials Science and Engineering, University of New South Wales, NSW 2052, Australia

[⊥]Research Center for Applied Sciences, Academia Sinica, Tin Ka Ping Photonics Center R517, 1001 Ta Hsueh Road, National Chiao Tung University, Hsinchu, Taiwan 300

ABSTRACT: In this work, we prepared few-layered graphene (FLG) films and investigated their thermoelectric properties. It was found that pristine FLG films showed a low thermopower of $\sim$40 μV/K. We further processed these FLG films by attaching them with 1,1′-azobis(cyanocyclohexane) or 1,3,6,8-pyrene-tetrasulfonic acid. The thermopower of FLG films with attached molecules increased to above $\sim$180 μV/K. Such enhancement in the thermopower led to an increase in their power factor by more than 4.5 times. Theoretical investigation indicated that a

potential difference can be introduced between the outer layer and inner layer of FLG films upon molecule attachments. Simulation of the thermopower based on Kubo's formula provided qualitative support to our experimental results.
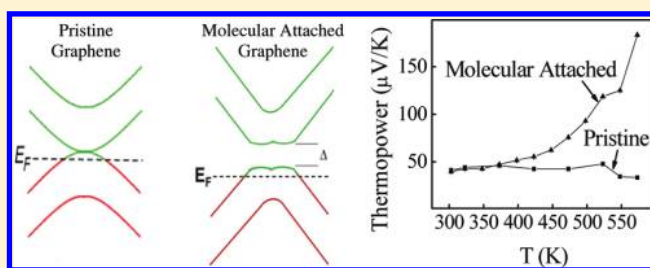
■ INTRODUCTION

Graphene, a single layer of carbon honeycomb lattice,[1] has attracted vast attention recently due to its unique properties. For instance, extremely high electronic mobility[2] ($\sim$200 000 cm^2/V·s),[3] high thermal conductivity ($\sim$5000 W/m·K),[4] ballistic transport,[5] and even magneto transport response.[6] There is enormous interest in tuning the electronic properties of graphene to expand their functionalities, for example, by chemical doping,[7] hydrogen attachment,[8] molecular attachments,[9−11] and so on. A variety of applications for graphene-based electronics have been proposed, such as single-molecular gas sensors,[12] spintronics,[13] high-speed transistors,[2,14] transparent electrodes,[15] and energy storage devices.[16−19] Besides the above-mentioned efforts, there is also interest in investigating their thermoelectric properties for thermoelectric energy conversion.[20−22] For thermoelectric materials, the efficiency is evaluated as a dimensionless figure of merit $ZT = S^2\sigma T/\kappa$, where T is the temperature in K, S is the thermopower, σ is the electrical conductivity, and κ is the thermal conductivity. Although there are theoretical predictions that ZT can be tuned to as high as >5.8,[23,24] the experimental demonstration of thermoelectric properties of graphene or even that including carbon nanotubes (CNTs) is not promising,[21,25−31] for instance, $ZT \approx 10^{-2}$. The factors that caused such low ZT values are mainly due to (1) the high lattice thermal conductivity and (2) the extremely low thermopower of graphene/CNTs. For the former issue, although pristine graphene/CNTs are well-known to possess high thermal conductivities,[4] there are several theoretical

works[24,32,33] that showed that the thermal conductivity of processed graphene can be reduced. In particular, zigzag graphene nanoribbons with disordered edges can reduce phonon thermal conductance by a few orders of magnitude.[24] For the latter issue, however, the reported maximum thermopower is only 40−50 μV/K.[21] Developing an engineering process that can significantly increase the thermopower without affecting much of the high electrical conductivities of graphene will then be a promising approach to open up possibility of using graphene for thermoelectric energy conversion, which can also contribute to the understanding of the intrinsic electrical properties of graphene.

Previously, the exploitation of using aromatic molecular doping on carbon materials has been well-reported.[9−11,34] Through such doping, the electron density distribution of pristine graphene can be altered as the aromatic molecule contains either electron-donating or electron-withdrawing groups that vary the electronic band structures.[9,11] Herein, we report a study on the temperature-dependent thermopower of molecule-attached chemical vapor deposition (CVD)-grown few-layered graphene (FLG) films up to 573 K. It was found that the pristine FLG films showed low thermopowers in the range of $\sim$40 μV/K, with electrical resistivities of 9×10^{-6}−2×10^{-5} Ω·m. Attaching the pristine graphene with two different molecules, for example, 1,1′-azobis(cyanocyclohexane)
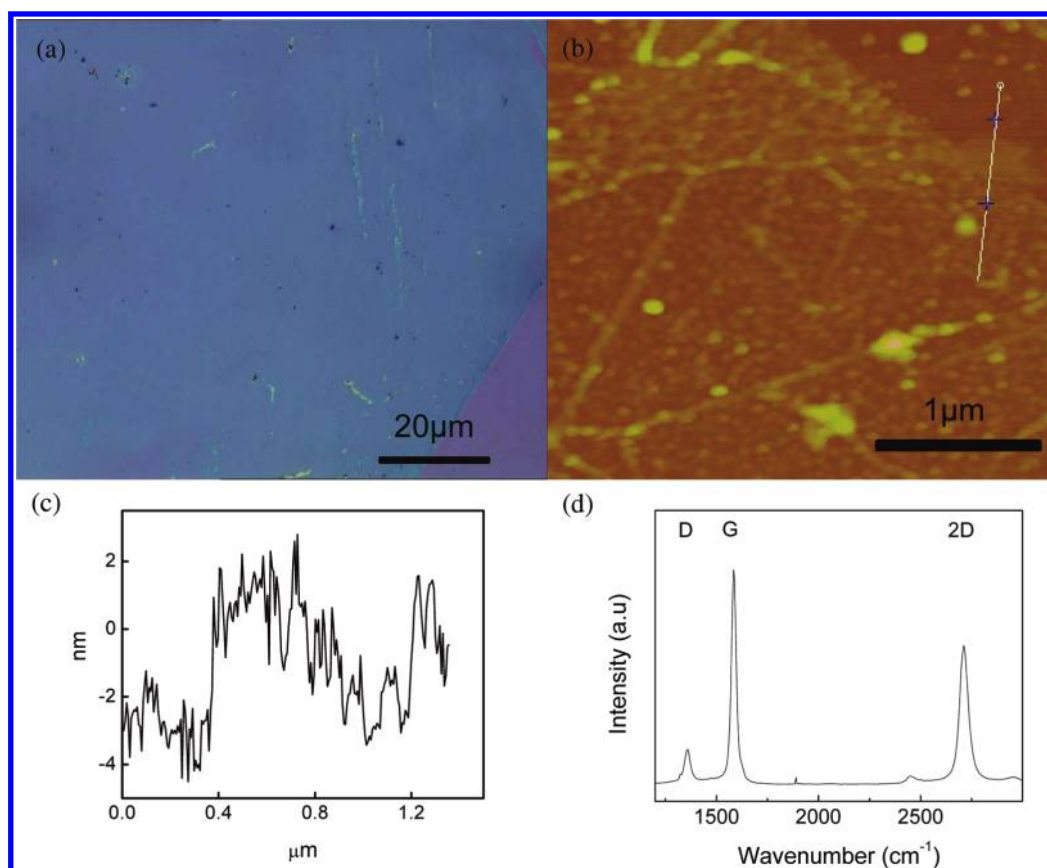
Figure 1. (a) Optical microscope image of a FLG film transferred to a SiO_2(300 nm)/Si substrate. (b) AFM image of the pristine FLG films on a SiO_2(300 nm)/Si substrate. (c) Cross-sectional height of the FLG measured. (d) Raman spectra of FLG tested using a 488 nm wavelength.

(ACN) and 1,3,6,8-pyrenetetrasulfonic acid (TPA), the S values increased to above 180 μV/K at 573 K, with electrical resistivities ranging from 3×10^{-5} to 4.5×10^{-5} $\Omega \cdot$m. Such enhancement in the thermopower of molecule-attached graphene may open the possibility to improve the thermoelectric performance toward the theoretical prediction.

■ EXPERIMENTAL SECTION

FLG films were first prepared by CVD process as reported[35] on a 50 μm thick copper foil (Alfa Aesar). The copper substrate was first heated to 1173 K under a 100 sccm argon/hydrogen (Ar/H_2) environment. A certain amount of organic precursor was then introduced for a few minutes at 1173 K. After the CVD growth, the foil was cooled down to ambient temperature under the Ar/H_2 environment. The FLG film on copper was removed from the furnace and then spin-coated with a layer of poly-methylmethaacrylate (PMMA). The copper foil was then etched away with iron nitrate solution, and the remaining film was floated on deionized water (DI H_2O). The film was then transferred to the desired substrates, and the PMMA was easily dissolved away using acetone. The FLG on the substrate was then blow-dried. Details of this technique will be addressed in a future publication. Substrates such as glass and silicon (1.5 cm $\times$ 1 cm) were washed with ethanol and DI water and subsequently dried.[36] The FLG films were then transferred to the glass and silicon substrates for further processing. Treatment was made to the pristine FLG by using ACN (98%) and TPA (85%) that was purchased from Aldrich. ACN was dissolved in *N*,*N*-dimethyl formamide

(DMF) solution with concentrations of 0.02 and 0.1 mol/L. Similarly, TPA was dissolved in DI H_2O with concentrations of 0.008 and 0.04 mol/L. After, the solutions were heated on a magnetic hot plate at 423 K for 30 min. It is reported that heating would dissociate ACN into two free radicals.[10] FLG films on substrates were then added into the respective solutions at 423 K for 15 min to allow interaction between the radicals and graphene. The FLG films on the substrates were subsequently removed and rinsed with either DMF (for ACN-attached samples) or DI H_2O (for TPA-attached samples) for 15 min. Finally, the FLG films were blow-dried.

Fourier transform infrared spectroscopy (FTIR) (Perkin-Elmer) was utilized to identify the bonding from samples. The spectrum obtained was scanned from 1500 to 500 cm^{-1} using the specular reflectance mode. WITec confocal Raman microscopy that used a 488 nm laser wavelength was employed to obtain Raman spectra of the samples. Reference from Si substrates at 520 cm^{-1} was used for calibration. Atomic force microscopy (AFM) (Digital Instruments) was used to determine the thickness of the FLG grown.

The thermopower and electrical resistivity (ρ) values (where resistivity is related to conductivity by $\sigma = 1/\rho$) were measured on pristine FLG films and treated FLG films from 300 to 573 K using a commercial ZEM 3 Seebeck meter. Before performing the measurement, the chamber was evacuated three times to remove ambient air and purged with helium gas. For comparison purpose, one set of pristine FLG films was first measured in the ZEM 3. Then, they were treated with 0.02 mol/L ACN in DMF solution. The treated FLG films were measured in the ZEM 3
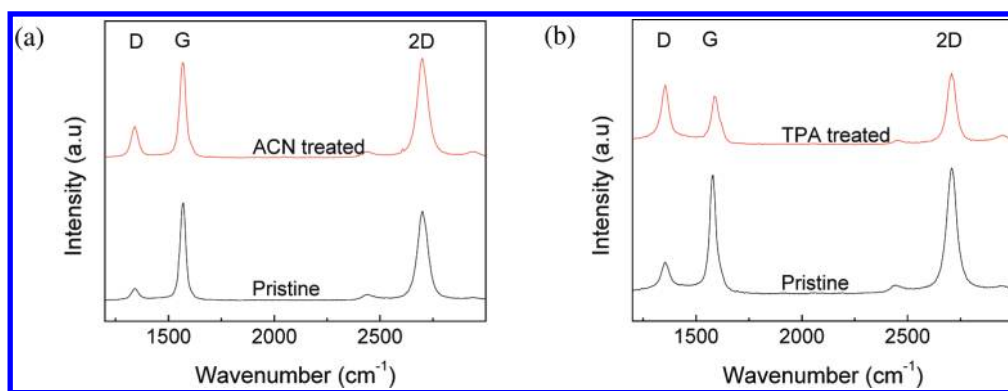
Figure 2. (a) Raman spectra of pristine FLG (bottom) and ACN-treated FLG (top). (b) Raman spectra of pristine FLG (bottom) and TPA-treated FLG (top).

again. The same treated FLG films were again treated with ACN in DMF solution with a higher concentration (0.1 mol/L) and tested in the ZEM 3. Another set of pristine FLG films were treated and tested in a similar way with TPA in DI H$_2$O solutions of different concentrations, with 0.008 and 0.04 mol/L.

■ RESULTS AND DISCUSSION

The optical image (see Figure 1a) showed that the pristine FLG films were continuous and were fairly uniform on the SiO$_2$(300 nm)/Si substrate. The AFM image (see Figure 1b) and the cross-sectional height profile (see Figure 1c) of the FLG films indicated that it was multilayered with a thickness of ~5 nm. In the Raman spectra of pristine FLG films (see Figure 1d), the relative intensity of the 2D band (located at 2710 cm^{-1}) with respect to that of the G band (located ~1584 cm^{-1}) was around ~1.1, indicating that these graphene films are multilayered.[37,38] A weak D band located at 1350 cm^{-1} was also observed in Figure 1d, which suggested the existence of structural defects in the graphene films.[37,39]

The Raman spectra of 0.1 mmol ACN-treated and 0.04 mmol TPA-treated FLG films were shown in Figure 2. In both cases, the intensity ratio between the D band and G band, $I(D)/I(G)$, increased after the treatments, which was evidence of the attachment. TPA attached to graphene by $\pi-\pi$ electron interaction, which caused an increase in the intensity of the D band after molecular treatment. In the case of ACN, it separated into two radicals upon heating. The radicals attached to graphene were similar to the functionalization process of CNT.[10,38] The intensity of the D band was enhanced because of the radical grafting. The peak positions of G and 2D bands in the Raman spectra of pristine, ACN-treated, and TPA-treated FLG films were summarized in Figure 3. Both ACN and TPA treatments lead to the upshifting of both G and 2D bands, suggesting the attachment of these molecules.[9]

The attachments of ACN and TPA onto the FLG films were also investigated by FTIR (see Figure 4). For ACN-treated FLG films, an absorption band at 1157 cm^{-1} could be attributed to the CN stretch. This observation suggested that ACN dissociates into two radicals through heating and the nitrogen group of the molecule functionalized with graphene. As for TPA-treated FLG films, an absorption band at 1143 cm^{-1}, corresponding to the diaryl sulfones, confirmed the successful attachment of TPA molecules.

The thermopower and electrical resistivities were investigated for the FLG films before and after the molecular attachment in the temperature range of 300−573 K (see Figure 5a,b). The pristine FLG films showed low S values of ~40 μV/K. The maximum values
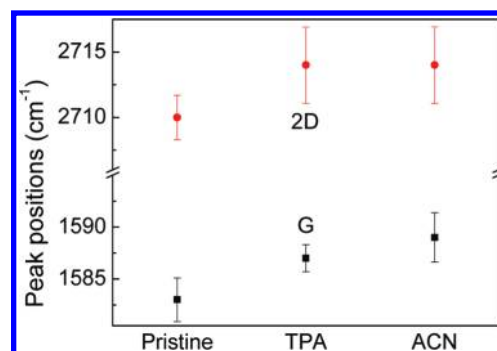

Figure 3. Raman G and 2D peak positions for pristine, ACN-treated, and TPA-treated FLG; error bars are drawn to specify the standard deviation of approximately 20 random measurements per sample.
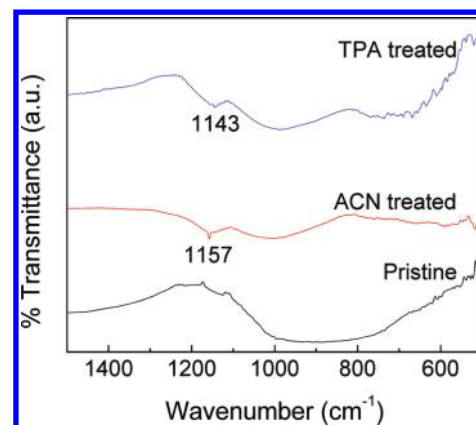

Figure 4. FTIR spectra of pristine, ACN-treated, and TPA-treated FLG.

of S increased for FLG films after treatment with ACN or TPA solutions of different concentrations. For example, FLG films treated with a 0.2 mol/L ACN solution showed maximum S values of ~125 μV/K at 573 K, which increased to ~180 μV/K for the same sample treated with an ACN solution of a higher concentration, 0.1 mol/L. Similarly, the maximum S values were amplified to ~70 and ~140 μV/K at 523 K for the FLG films treated with 0.008 and 0.04 mol/L TPA in DI H$_2$O solutions, respectively.

Upon treatment with ACN and TPA solutions, the electrical conductivities of the FLG films decreased (see Figure 5c,d), although it was reported that attachment of aromatic molecules
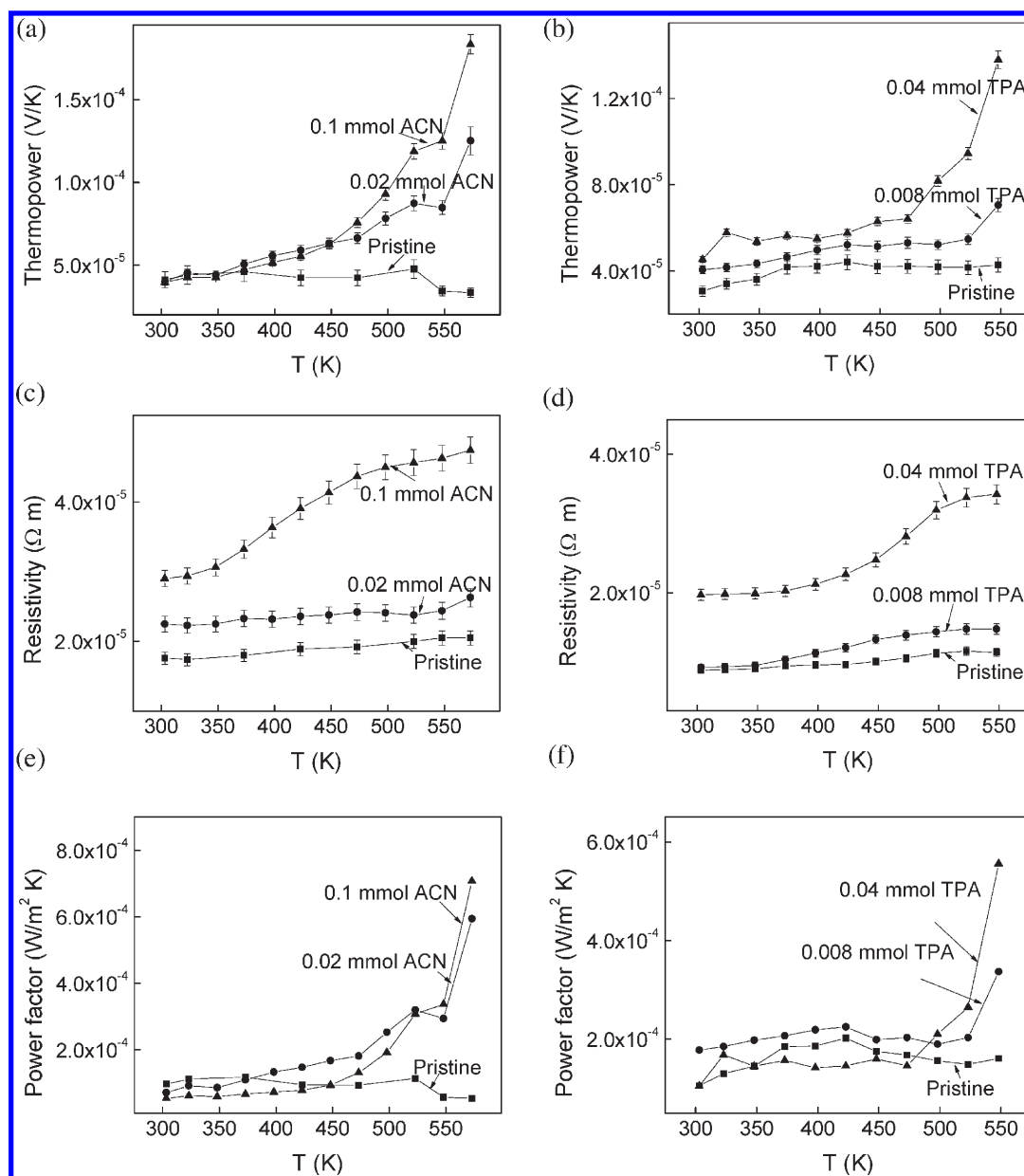
Figure 5. Thermopower (a, b), resistivity (c, d), and power factor (e, f) of pristine FLG and different concentrations of ACN- and TPA-treated FLG.

led to an increase in electrical conductivities through doping of the graphene films.[9] The measured ρ values of pristine FLG films were in the range of $9 \times 10^{-6} - 2 \times 10^{-5}\ \Omega \cdot m$ in the temperature range of 300–573 K, which was comparable to those previously reported.[40] Upon treatment with the molecule solutions, the electrical resistivities of the graphene films increased slightly within the same order of magnitude, for example, to $3 \times 10^{-5} - 4.5 \times 10^{-5}\ \Omega \cdot m$ after treatment with the 0.1 mol/L ACN solution and to $2 \times 10^{-5} - 3.5 \times 10^{-5}\ \Omega \cdot m$ after treatment with the 0.04 mol/L TPA solution. Although the electrical resistivity increased for FLG films upon molecule attachments, the maximum power factor increased, for example, by 7 times for 0.1 mol/L ACN solution treatment and by 4.5 times for 0.04 mol/L TPA solution treatment (see Figure 5e,f). In terms of thermal conductivity of the FLG, we expected the value to reduce with the molecular attachment. Several theoretical studies have

been reported to show a reduction in thermal conductivity, for instance, through defect generation[23] and isotope doping[33] in graphene. In our molecular-attached FLG, the increment in the D band (Figure 2a,b) provided disorder to the outer layers of the graphene, which could act as phonon scattering sites to reduce the lattice thermal conductivity.

To understand the role of molecular attachment on graphene and the enhancement in S, we analyzed a bilayer graphene through Bernal stacking. A tight-binding Hamiltonian model for the Pz band with the nearest-neighboring intralayer and interlayer hopping terms is written as[41,42]

$$H_0 = \sum_{k\sigma} [T(k)(a_{1k\sigma}^+ b_{1k\sigma} + a_{2k\sigma}^+ b_{2k\sigma}) + t_\perp (b_{1k\sigma}^+ a_{2k\sigma} + b_{2k\sigma}^+ a_{1k\sigma})$$

$$+ \text{h.c.}] + \frac{V}{2}(a_{1k\sigma}^+ a_{1k\sigma} + b_{1k\sigma}^+ b_{1k\sigma} - a_{2k\sigma}^+ a_{2k\sigma} - b_{2k\sigma}^+ b_{2k\sigma})$$
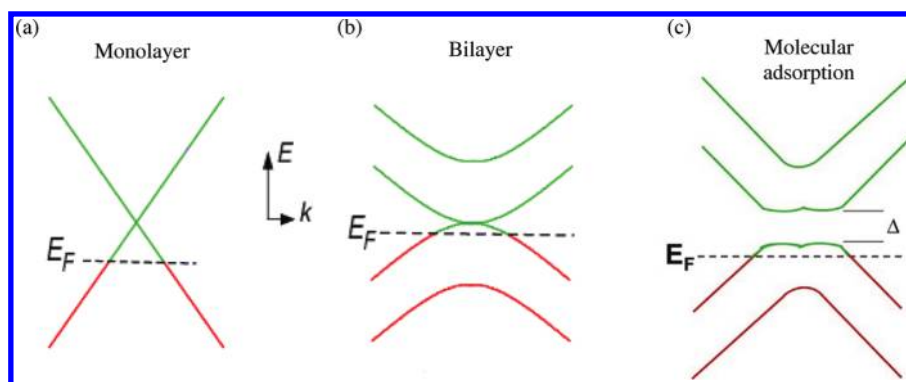
1783

dx.doi.org/10.1021/jp1103609 |*J. Phys. Chem. C* 2011, 115, 1780–1785

Figure 6. Schematic diagram of the electronic structure of (a) monolayer and (b) bilayer graphene and (c) molecular attached bilayer graphene.

with

$$T(k) = -t\left[\cos k_x a + 2\cos\left(\frac{k_x a}{2}\right)\cos\left(\frac{\sqrt{3}k_y a}{2}\right)\right.$$
$$\left. + i\left(-\sin k_x a + 2\sin\left(\frac{k_x a}{2}\right)\cos\left(\frac{\sqrt{3}k_y a}{2}\right)\right)\right]$$

where $t \approx 3.0$ eV is the intralayer nearest-neighbor hopping energy between the different sublattices A and B and $t_\perp \approx 0.3$ eV is the next-nearest-neighbor interlayer hopping energy; $a = 1.42$ Å is the nearest-neighbor interplayer carbon—carbon bond length, and V is the potential energy difference between the first and second layers induced by the charged molecules adsorbed on the surface of the graphene. Here, $a_{1k\sigma}^+$ and $b_{1k\sigma}^+$ denote creation of $\alpha(=1,2)$ layer states with wave vector k and spin σ on the A and B sublattice, respectively.

The energy band derived from the Hamiltonian has the following forms

$$E_{1+} = \frac{1}{\sqrt{2}}$$
$$\sqrt{\frac{V^2}{2} + t_\perp^2 + 2T^*(k)T(k) + \sqrt{t_\perp^4 + 4T^*(k)T(k)(V^2 + t_\perp^2)}}$$

$$E_{2+} = \frac{1}{\sqrt{2}}$$
$$\sqrt{\frac{V^2}{2} + t_\perp^2 + 2T^*(k)T(k) - \sqrt{t_\perp^4 + 4T^*(k)T(k)(V^2 + t_\perp^2)}}$$

$$E_{1-} = -\frac{1}{\sqrt{2}}$$
$$\sqrt{\frac{V^2}{2} + t_\perp^2 + 2T^*(k)T(k) + \sqrt{t_\perp^4 + 4T^*(k)T(k)(V^2 + t_\perp^2)}}$$

$$E_{2-} = -\frac{1}{\sqrt{2}}$$
$$\sqrt{\frac{V^2}{2} + t_\perp^2 + 2T^*(k)T(k) - \sqrt{t_\perp^4 + 4T^*(k)T(k)(V^2 + t_\perp^2)}}$$

where the positive sign represents the conduction band and the negative sign represents the valence band, with $E_{1+} > E_{2+} > E_{2-} > E_{1-}$

Figure 6a,b shows the schematic diagram of the difference in the electronic band structure of monolayer and bilayer graphene
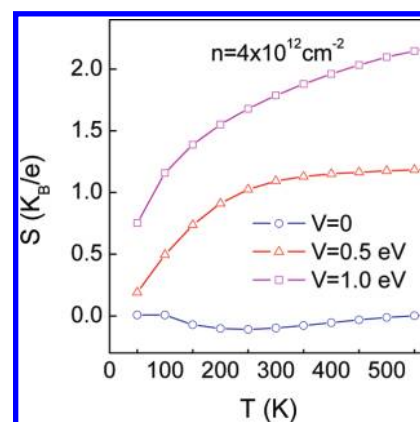

Figure 7. Calculated thermopower of treated FLG in different voltage potentials induced by the molecular absorption.

with $V = 0$. We used a bilayer graphene band structure, instead of a monolayer model, to explain our results as it relates closer to our FLG samples. Due to the asymmetry in the bilayer graphene with $V \neq 0$, a gap can be introduced (see Figure 6c) as the outer-layer and innerlayer graphene molecular adsorptions are different and lead to the potential difference between them.[42] Notice that to simplify the model, we neglect the changes of hopping energy t, the interlayer hopping $t_\perp$, and the gap open due to hole doping,[43] defects,[44] and/or interlayer[41,42] interaction upon attachment of the molecule on the FLG films.

The calculation for thermopower is based on Kubo's formula,[45] and the current—current correlation functions are used as reference.[46] Hall measurements on the FLG samples showed a carrier density with a magnitude of 10^{12}—10^{13}. Figure 7 shows the results of the calculated thermopower versus temperature for several values of V induced by the molecules adsorbed on the surface of the FLG samples. (Note that the thermopower coefficient S is in units of K_B/e, 1 $K_B/e \approx 86$ $\mu V/K$.) It is shown that the increased surface potential leads to enhancement of the thermopower, which gives qualitative support to our experimental observation.

■ CONCLUSIONS

In summary, we investigated the thermoelectric properties of ACN- or TPA-treated FLG films. It was shown that the maximum thermopower of the FLG films after molecular attachment can reach above 180 $\mu V/K$, as compared to only 40 $\mu V/K$ for the pristine ones. Although the electrical resistivities increased slightly for the samples after ACN or TPA treatments, the power

factors were able to increase by 7 times (e.g., 0.1 mmol ACN solution treatment) and 4.5 times (e.g., 0.04 mmol TPA solution treatment), respectively. We proposed that the attachment of the molecules on the FLG led to the variation of the surface potential and the opening of the band gap, which was investigated through the tight-binding Hamiltonian model. The simulated curves of the thermopower provided qualitative support to our hypothesis.

■ AUTHOR INFORMATION

Corresponding Author

*E-mail: alexyan@ntu.edu.sg. Tel: +65 6790 4583. Fax: +65 6790 9081 (Q.Y.); E-mail: ashhhng@ntu.edu.sg. Tel: +65 6790 4140. Fax: +65 6790 9081 (H.H.H.).

■ ACKNOWLEDGMENT

■ REFERENCES

(1) Geim, A. K.; Novoselov, K. S. *Nat. Mater.* **2007**, *6*, 183.

(2) Novoselov, K. S.; Geim, A. K.; Morozov, S. V.; Jiang, D.; Zhang, Y.; Dubonos, S. V.; Grigorieva, I. V.; Firsov, A. A. *Science* **2004**, *306*, 666.

(3) Bolotin, K. I.; Sikes, K. J.; Jiang, Z.; Klima, M.; Fudenberg, G.; Hone, J.; Kim, P.; Stormer, H. L. *Solid State Commun.* **2008**, *146*, 351.

(4) Balandin, A. A.; Ghosh, S.; Bao, W.; Calizo, I.; Teweldebrhan, D.; Miao, F.; Lau, C. N. *Nano Lett.* **2008**, *8*, 902.

(5) Du, X.; Skachko, I.; Barker, A.; Andrei, E. Y. *Nat. Nano* **2008**, *3*, 491.

(6) Zhang, Y.; Tan, Y.-W.; Stormer, H. L.; Kim, P. *Nature* **2005**, *438*, 201.

(7) Wang, X. R.; Li, X. L.; Zhang, L.; Yoon, Y.; Weber, P. K.; Wang, H. L.; Guo, J.; Dai, H. J. *Science* **2009**, *324*, 768.

(8) Elias, D. C.; Nair, R. R.; Mohiuddin, T. M. G.; Morozov, S. V.; Blake, P.; Halsall, M. P.; Ferrari, A. C.; Boukhvalov, D. W.; Katsnelson, M. I.; Geim, A. K.; Novoselov, K. S. *Science* **2009**, *323*, 610.

(9) Xiaochen, D.; Dongliang, F.; Wenjing, F.; Yumeng, S.; Peng, C.; Lain-Jong, L. *Small* **2009**, *5*, 1422.

(10) Zhao, J.; Lee, C. W.; Han, X.; Chen, F.; Xu, Y.; Huang, Y.; Chan-Park, M. B.; Chen, P.; Li, L.-J. *Chem. Commun.* **2009**, *46*, 7182.

(11) Dong, X.; Shi, Y.; Zhao, Y.; Chen, D.; Ye, J.; Yao, Y.; Gao, F.; Ni, Z.; Yu, T.; Shen, Z.; Huang, Y.; Chen, P.; Li, L.-J. *Phys. Rev. Lett.* **2009**, *102*, 135501.

(12) Schedin, F.; Geim, A. K.; Morozov, S. V.; Hill, E. W.; Blake, P.; Katsnelson, M. I.; Novoselov, K. S. *Nat. Mater.* **2007**, *6*, 652.

(13) Kane, C. L.; Mele, E. J. *Phys. Rev. Lett.* **2005**, *95*, 226801.

(14) Wang, X.; Li, X.; Zhang, L.; Yoon, Y.; Weber, P. K.; Wang, H.; Guo, J.; Dai, H. *Science* **2009**, *324*, 768.

(15) Zhao, J.; Pei, S.; Ren, W.; Gao, L.; Cheng, H.-M. *ACS Nano* **2010**, *4*, 5245.

(16) Murugan, A. V.; Muraliganth, T.; Manthiram, A. *Chem. Mater.* **2009**, *21*, 5004.

(17) Wang, Y.; Shi, Z.; Huang, Y.; Ma, Y.; Wang, C.; Chen, M.; Chen, Y. *J. Phys. Chem. C* **2009**, *113*, 13103.

(18) Zhao, X.; Tian, H.; Zhu, M.; Tian, K.; Wang, J. J.; Kang, F.; Outlaw, R. A. *J. Power Sources* **2009**, *194*, 1208.

(19) Liang, M.; Zhi, L. *J. Mater. Chem.* **2009**, *19*, 5871.

(20) Zuev, Y. M.; Chang, W.; Kim, P. *Phys. Rev. Lett.* **2009**, *102*, 096807.

(21) Wei, P.; Bao, W. Z.; Pu, Y.; Lau, C. N.; Shi, J. *Phys. Rev. Lett.* **2009**, *102*, 166808.

(22) Checkelsky, J. G.; Ong, N. P. *Phys. Rev. B* **2009**, *80*, 081413.

(23) Ni, X. X.; Liang, G. C.; Wang, J. S.; Li, B. W. *Appl. Phys. Lett.* **2009**, *95*, 192114.

(24) Sevincli, H.; Cuniberti, G. *Phys. Rev. B* **2010**, *81*, 113401.

(25) Xing, Y. X.; Sun, Q. F.; Wang, J. *Phys. Rev. B* **2009**, *80*, 235411.

(26) Dragoman, D.; Dragoman, M. *Appl. Phys. Lett.* **2007**, *91*, 173117.

(27) Zhu, L. J.; Ma, R.; Sheng, L.; Liu, M.; Sheng, D. N. *Phys. Rev. Lett.* **2010**, *104*, 076804.

(28) Kong, W. J.; Lu, L.; Zhu, H. W.; Wei, B. Q.; Wu, D. H. *J. Phys.: Condens. Matter* **2005**, *17*, 1923.

(29) Sumanasekera, G. U.; Pradhan, B. K.; Romero, H. E.; Adu, K. W.; Eklund, P. C. *Phys. Rev. Lett.* **2002**, *89*, 166801.

(30) Romero, H. E.; Sumanasekera, G. U.; Mahan, G. D.; Eklund, P. C. *Phys. Rev. B* **2002**, *65*, 205410.

(31) Yao, Q.; Chen, L. D.; Zhang, W. Q.; Liufu, S. C.; Chen, X. H. *ACS Nano* **2010**, *4*, 2445.

(32) Li, X.; Maute, K.; Dunn, M. L.; Yang, R. *Phys. Rev. B* **2010**, *81*, 245318.

(33) Mingo, N.; Esfarjani, K.; Broido, D. A.; Stewart, D. A. *Phys. Rev. B* **2010**, *81*, 045408.

(34) Kanungo, M.; Lu, H.; Malliaras, G. G.; Blanchet, G. B. *Science* **2009**, *323*, 234.

(35) Srivastava, A.; Galande, C.; Ci, L.; Song, L.; Rai, C.; Jariwala, D.; Kelly, K. F.; Ajayan, P. M. *Chem. Mater.* **2010**, *22*, 3457.

(36) Chen, J.; Sun, T.; Sim, D.; Peng, H.; Wang, H.; Fan, S.; Hng, H. H.; Ma, J.; Boey, F. Y. C.; Li, S.; Samani, M. K.; Chen, G. C. K.; Chen, X.; Wu, T.; Yan, Q. *Chem. Mater.* **2010**, *22*, 3086.

(37) Tuinstra, F.; Koenig, J. L. *J. Chem. Phys.* **1970**, *53*, 1126.

(38) Stoffelbach, F.; Aqil, A.; Jerome, C.; Jerome, R.; Detrembleur, C. *Chem. Commun.* **2005**, *36*, 4532.

(39) Allen, M. J.; Tung, V. C.; Kaner, R. B. *Chem. Rev.* **2009**, *110*, 132.

(40) Reina, A.; Jia, X.; Ho, J.; Nezich, D.; Son, H.; Bulovic, V.; Dresselhaus, M. S.; Kong, J. *Nano Lett.* **2008**, *9*, 30.

(41) Guinea, F.; Castro Neto, A. H.; Peres, N. M. R. *Phys. Rev. B* **2006**, *73*, 245426.

(42) McCann, E. *Phys. Rev. B* **2006**, *74*, 161403.

(43) Ohta, T.; Bostwick, A.; Seyller, T.; Horn, K.; Rotenberg, E. *Science* **2006**, *313*, 951.

(44) Lofwander, T.; Fogelstrom, M. *Phys. Rev. B* **2007**, *76*, 4.

(45) Jonson, M.; Mahan, G. D. *Phys. Rev. B* **1980**, *21*, 4223.

(46) Palsson, G.; Kotliar, G. *Phys. Rev. Lett.* **1998**, *80*, 4775.

1785

dx.doi.org/10.1021/jp1103609 |*J. Phys. Chem. C* 2011, 115, 1780–1785